J|A|C|S COMMUNICATIONS

Published on Web 09/20/2010

Mn_3O_4−Graphene Hybrid as a High-Capacity Anode Material for Lithium Ion Batteries

Hailiang Wang,[†,§] Li-Feng Cui,[‡,§] Yuan Yang,[‡] Hernan Sanchez Casalongue,[†] Joshua Tucker Robinson,[†] Yongye Liang,[†] Yi Cui,[*,‡] and Hongjie Dai[*,†]

Department of Chemistry and Laboratory for Advanced Materials and Department of Materials Science and Engineering, Stanford University, Stanford, California 94305

Received June 17, 2010; E-mail: hdai@stanford.edu; yicui@stanford.edu

Abstract: We developed two-step solution-phase reactions to form hybrid materials of Mn_3O_4 nanoparticles on reduced graphene oxide (RGO) sheets for lithium ion battery applications. Selective growth of Mn_3O_4 nanoparticles on RGO sheets, in contrast to free particle growth in solution, allowed for the electrically insulating Mn_3O_4 nanoparticles to be wired up to a current collector through the underlying conducting graphene network. The Mn_3O_4 nanoparticles formed on RGO show a high specific capacity up to ∼900 mAh/g, near their theoretical capacity, with good rate capability and cycling stability, owing to the intimate interactions between the graphene substrates and the Mn_3O_4 nanoparticles grown atop. The Mn_3O_4/RGO hybrid could be a promising candidate material for a high-capacity, low-cost, and environmentally friendly anode for lithium ion batteries. Our growth-on-graphene approach should offer a new technique for the design and synthesis of battery electrodes based on highly insulating materials.

Nanomaterials of metal oxides, such as Co_3O_4,[1,2] SnO_2,[3] FeO_x,[1,4] and NiO,[1] have been intensively studied as anode materials for lithium ion batteries (LIBs) aimed at achieving higher specific capacities than graphite. For instance, nanocrystals of Co_3O_4 have been synthesized for LIB anodes with specific capacities ∼2 times that of graphite, affording LIBs with higher energy density.[1,2] Compared to Co_3O_4, Mn_3O_4 is an attractive anode material for LIBs due to the high abundance of Mn, low cost, and environmental benignity. However, little has been done thus far in utilizing Mn_3O_4 as an anode material,[5,6] partly due to its extremely low electrical conductivity (∼10^{-7}−10^{-8} S/cm), limiting its capacity to ≤ ∼400 mAh/g even with Co doping,[6] well below the theoretical capacity of ∼936 mAh/g. It is highly desirable to increase the capacity of Mn_3O_4 by electrically wiring up Mn_3O_4 nanoparticles to an underlying conducting substrate.

Graphene is an excellent substrate to host active nanomaterials for energy applications due to its high conductivity, large surface area, flexibility, and chemical stability. We have shown recently that the specific capacitance and power rate of $Ni(OH)_2$ could be enhanced by growing $Ni(OH)_2$ nanoplates on graphene sheets, useful for supercapacitor applications.[7] Co_3O_4−graphene and Fe_3O_4−graphene composite materials have also been recently prepared as anode materials of LIBs,[8] with performance comparable to that of previously reported Co_3O_4- and Fe_3O_4-based anodes.[2a,c,4a,c] It is more challenging to explore Mn_3O_4−graphene hybrid materials due to the much lower conductivity of Mn_3O_4 than Co_3O_4 and Fe_3O_4.

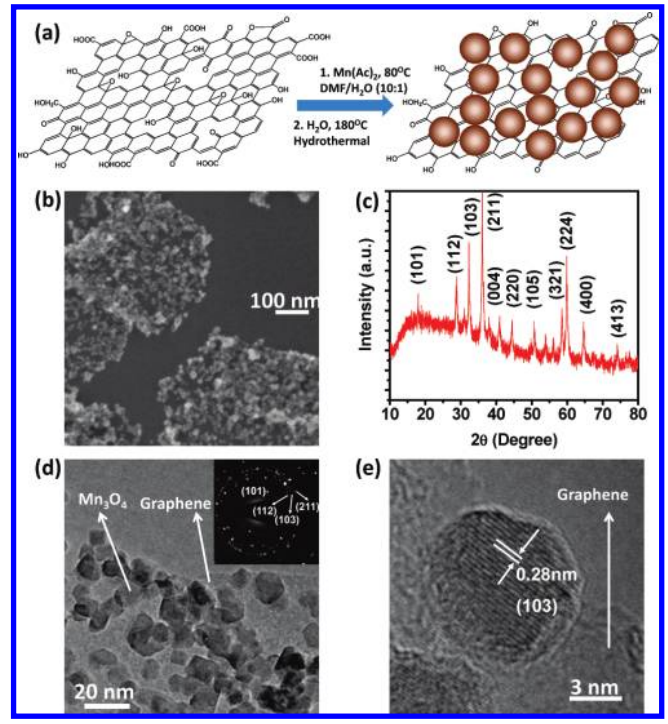

Figure 1. Mn_3O_4 nanoparticles grown on GO. (a) Schematic two-step synthesis of Mn_3O_4/RGO. (b) SEM image of Mn_3O_4/RGO hybrid. (c) XRD spectrum of a packed thick film of Mn_3O_4/RGO. (d) TEM image of Mn_3O_4/RGO; inset shows the electron diffraction pattern of the Mn_3O_4 nanoparticles on RGO. (e) High-resolution TEM image of an individual Mn_3O_4 nanoparticle on RGO.

Here, we report a two-step solution-phase method for growing Mn_3O_4 nanoparticles on graphene oxide (GO) to form a Mn_3O_4−reduced GO (RGO) hybrid material. The Mn_3O_4/RGO hybrid afforded an unprecedented high capacity of ∼900 mAh/g based on the mass of Mn_3O_4 (∼810 mAh/g based on the total mass of the hybrid), with good rate capability and cycling stability. This growth-on-graphene approach would be very useful in boosting the electrochemical performance of highly insulating electrode materials.

Mn_3O_4 nanoparticles were grown on GO sheets by a two-step solution-phase reaction scheme [Figure 1, also see Supporting Information (SI) for details] recently developed for the synthesis of a $Ni(OH)_2$/graphene hybrid and a TiO_2/graphene hybrid.[7] GO used in this work was prepared by a modified Hummers method (SI),[9] in which a 6 times lower concentration of $KMnO_4$ was used (see SI) to result in GO sheets with lower oxygen content than Hummers's GO (∼15% vs ∼30% measured by XPS and Auger spectroscopy).

In the first step, hydrolysis of $Mn(CH_3COO)_2$ in a GO suspension with a 10:1 *N*,*N*-dimethylformamide (DMF)/H_2O mixed solvent at

[†] Department of Chemistry and Laboratory for Advanced Materials.
[‡] Department of Materials Science and Engineering.
[§] These authors contributed equally to this work.

10.1021/ja105296a

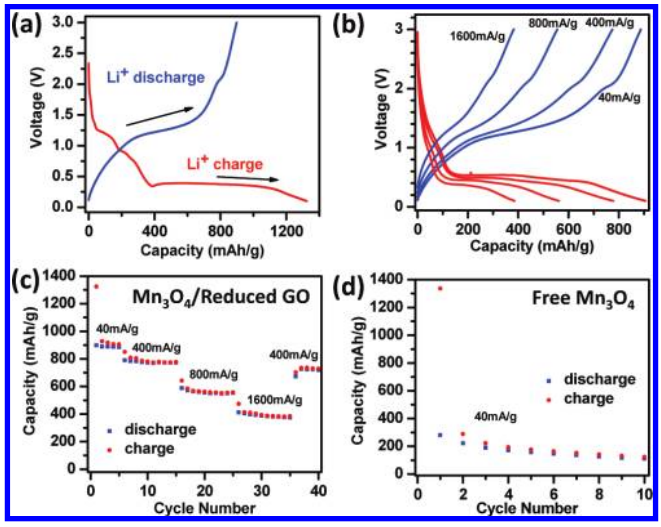

Figure 2. Electrochemical characterizations of a half-cell composed of Mn_3O_4/RGO and Li. The specific capacities are based on the mass of Mn_3O_4 in the Mn_3O_4/RGO hybrid. (a) Charge (red) and discharge (blue) curves of Mn_3O_4/RGO for the first cycle at a current density of 40 mA/g. (b) Representative charge (red) and discharge (blue) curves of Mn_3O_4/RGO at various current densities. (c) Capacity retention of Mn_3O_4/RGO at various current densities. (d) Capacity retention of free Mn_3O_4 nanoparticles without graphene at a current density of 40 mA/g.

80 °C afforded a dense and uniform coating with small and poorly crystalline precursor nanoparticles on GO (see SI and Figure S1). The mixed solvent and low temperature were important to control the hydrolysis reaction at a low rate to avoid particle formation in free solution. It is possible that nanoparticles grown this way were anchored covalently to GO through functional groups such as carboxyl, hydroxyl, and epoxy groups on the surface of GO sheets.

The product from the first step was then transferred to deionized water and treated in hydrothermal conditions at 180 °C for 10 h, which afforded well-crystallized Mn_3O_4 nanoparticles uniformly distributed on RGO sheets (Figure 1), with ~10 wt % RGO in the hybrid material. Through the synthesis, the starting GO sheets evolved into RGO due to the hydrothermal treatment at 180 °C, as evidenced by the red shift of the absorption peak in UV−vis spectra (SI, Figure S2).[10] The size of the Mn_3O_4 nanoparticles was ~10−20 nm, as revealed by the scanning electron microscopy (SEM) and transmission electron microscopy (TEM) images (Figure 1b,d), which was consistent with the width of the diffraction peaks in the XRD spectrum (Figure 1c). The high-resolution TEM image (Figure 1e) showed the crystal lattice fringes throughout the entire Mn_3O_4 nanoparticle formed on RGO.

The Mn_3O_4/RGO hybrid material was mixed with carbon black and polyvinyldifluoride (PVDF) in a weight ratio of 80:10:10 for preparing a working electrode. The electrochemical measurements were carried out in coin cells with a Li foil as the counter electrode and 1 M $LiPF_6$ in 1:1 ethylene carbonate (EC) and diethyl carbonate (DEC) as the electrolyte. Figure 2a shows the charge and discharge curves of the Mn_3O_4/RGO anode for the first cycle at a current density of 40 mA/g and cycled between 3.0 and 0.1 V vs Li^+/Li. The capacity corresponding to the voltage range of ~1.2−0.4 V of the first Li^+ charge curve was due to irreversible reactions between Li^+ and RGO and decomposition of the electrolyte solvent, forming a solid electrolyte interphase.[11] The voltage plateau at ~0.4 V reflected the Li^+ charge reaction: $Mn_3O_4 + 8Li^+ + 8e^- \rightarrow 3Mn(0) + 8Li_2O$.[8b] The discharge curve showed a sloping plateau at ~1.2 V due to the reverse reaction. After several conditioning cycles, the Coulombic efficiency of the coin cell increased to higher than 98% (Figure 2b,c), indicating good reversibility of the above conversion reaction between Mn_3O_4 and Mn(0). The charge capacity in the range of 1.2−0.4 V was mainly due to reduction from Mn(III) to Mn(II), and the 0.4−0.1 V range reflected the reduction from Mn(II) to Mn(0).[6] Little charge capacity would have been obtained in the range of 1.2−0.5 V if the electrode had been cycled between Mn(II) and Mn(0).[6] This further verified the conversion reaction we suggested above.

Figure 2b shows representative charge and discharge voltage profiles of the Mn_3O_4/RGO anode at various current densities (see SI, Figure S4 for other data sets). With the increase of current density, the charge potential of the Mn_3O_4/RGO anode decreased and the discharge potential increased, rendering higher overpotential. The cell was first cycled at a low current density of 40 mA/g for five cycles, where a stable specific capacity of ~900 mAh/g (Figure 2c) was obtained, based on the mass of the Mn_3O_4 nanoparticles in the Mn_3O_4/RGO hybrid (~810 mAh/g based on the total mass of the hybrid), which was very close to the theoretical capacity of ~936 mAh/g for Mn_3O_4 based on the conversion reaction above. This is also the highest capacity that has been reported for Mn_3O_4 anode materials. To our knowledge, previously, the highest capacity with similar cycle stability for Mn_3O_4 anode was ~500 mAh/g at ~33−50 mA/g.[6] Our Mn_3O_4 nanoparticles formed on RGO showed good rate performance as well. The capacity was as high as ~780 mAh/g after we increased the current density by 10 times. Even at a high current density of 1600 mA/g, the specific capacity was ~390 mAh/g, still higher than the theoretical capacity of graphite (~372 mAh/g). A capacity of ~730 mAh/g at 400 mA/g was retained after 40 cycles of charge and discharge at various current densities (Figure 2c), indicating good cycling stability (cycling data up to 150 cycles available in Figure S4).

The high capacity and rate capability and good cycling stability of our Mn_3O_4/RGO hybrid material were attributed to the intimate interaction between the graphene substrates and the Mn_3O_4 nanoparticles directly grown on them, which made Mn_3O_4 electrochemically active since charge carriers could be effectively and rapidly conducted back and forth from the Mn_3O_4 nanoparticles to the current collector through the highly conducting three-dimensional graphene network. The graphene−nanoparticle interaction also afforded a good dispersion of the Mn_3O_4 nanoparticles grown on the RGO sheets to avoid aggregation (Figure S5), desired for cycle stability.

In a control experiment, we synthesized free Mn_3O_4 nanoparticles by the same two-step method without any graphene added (SI). Although the free Mn_3O_4 nanoparticles had morphology, size, and crystallinity similar to those of nanoparticles formed on RGO sheets (Figure S3), the electrochemical performance of these free Mn_3O_4 nanoparticles physically mixed with carbon black was much worse than that of the Mn_3O_4/RGO hybrid material mixed with carbon black. At a low current density of 40 mA/g, the free Mn_3O_4 nanoparticles showed a capacity lower than 300 mAh/g, which further decreased to ~115 mAh/g after only 10 cycles (Figure 2d).

In conclusion, by selectively growing Mn_3O_4 nanoparticles on graphene oxide to form Mn_3O_4/RGO hybrid, we enabled a highly insulating material Mn_3O_4 to approach its theoretical capacity as an anode material for LIBs. The Mn_3O_4−graphene hybrid could be further explored for high-capacity, low-cost, and nontoxic anode material for battery applications. Our growth-on-graphene approach should also offer an effective and convenient technique to improve the specific capacities and rate capabilities of highly insulating electrode materials in the battery area.

Acknowledgment. This work was supported in part by the Office of Naval Research, NSF award CHE-0639053 and a KAUST

Investigator Award H. Wang and Y. Yang acknowledge financial support from Stanford Graduate Fellowship.

Supporting Information Available: Experimental details and supplementary figures. This material is available free of charge via the Internet at http://pubs.acs.org.

References

(1) Poizot, P.; Laruelle, S.; Grugeon, S.; Dupont, L.; Tarascon, J.-M. *Nature* **2000**, *407*, 496–499.
(2) (a) Nam, K. T.; Kim, D. P.; Yoo, J.; Chiang, C.; Meethong, N.; Hammond, P. T.; Chiang, Y.; Belcher, A. M. *Science* **2006**, *312*, 885–888. (b) Lou, X. W.; Deng, D.; Lee, J. Y.; Feng, J.; Archer, L. A. *Adv. Mater.* **2008**, *20*, 258–262. (c) Li, Y.; Tan, B.; Wu, Y. *Nano Lett.* **2008**, *8*, 265–270.
(3) (a) Meduri, P.; Pendyala, C.; Kumar, V.; Sumanasekera, G. U.; Sunkara, M. K. *Nano Lett.* **2009**, *9*, 612–616. (b) Ye, J.; Zhang, H.; Yang, R.; Li, X.; Qi, L. *Small* **2010**, *6*, 296–306.
(4) (a) Ban, C.; Wu, Z.; Gillaspie, D. T.; Chen, L.; Yan, Y.; Blackburn, J. L.; Dillon, A. C. *Adv. Mater.* **2010**, *22*, E145–E149. (b) Zhong, J.; Cao, C.; Liu, Y.; Li, Y.; Khan, W. S. *Chem. Commun.* **2010**, *46*, 3869–3871. (c) Wang, S.; Zhang, J.; Chen, C. *J. Power Sources* **2010**, *195*, 5379–5381.
(5) Fan, Q.; Whittingham, M. S. *Mater. Res. Soc. Symp. Proc.* **2007**, *972*, 0972-AA07-03-BB08-03.
(6) Pasero, D.; Reeves, N.; West, A. R. *J. Power Sources* **2005**, *141*, 156–158.
(7) (a) Wang, H.; Robinson, J. T.; Diankov, G.; Dai, H. *J. Am. Chem. Soc.* **2010**, *132*, 3270–3271. (b) Wang, H.; Sanchez Casalongue, H.; Liang, Y.; Dai, H. *J. Am. Chem. Soc.* **2010**, *132*, 7472–7477. (c) Liang, Y.; Wang, H.; Sanchez Casalongue, H.; Chen, Z.; Dai, H. *Nano Res.* **2010**, *3*, 701–705.
(8) (a) Yang, S.; Cui, G.; Pang, S.; Cao, Q.; Kolb, U.; Feng, X.; Maier, J.; Mullen, K. *ChemSusChem* **2010**, *3*, 236–239. (b) Wu, Z.; Ren, W.; Wen, L.; Gao, L.; Zhao, J.; Chen, Z.; Zhou, G.; Li, F.; Cheng, H. *ACS Nano* **2010**, *4*, 3187–3194. (c) Zhang, M.; Lei, D.; Yin, X.; Chen, L.; Li, Q.; Wang, Y.; Wang, T. *J. Mater. Chem.* **2010**, *20*, 5538–5543. (d) Zhou, G.; Wang, D.; Li, F.; Zhang, L.; Li, N.; Wu, Z.; Wen, L.; Lu, G. Q.; Cheng, H. *Chem. Mater.* **2010**, in press (DOI: 10.1021/cm101532x).
(9) (a) Hummers, W. S.; Offeman, R. E. *J. Am. Chem. Soc.* **1958**, *80*, 1339–1339. (b) Wang, H.; Wang, X.; Li, X.; Dai, H. *Nano Res.* **2009**, *2*, 336–342. (c) Sun, X.; Liu, Z.; Welsher, K.; Robinson, J. T.; Goodwin, A.; Zaric, S.; Dai, H. *Nano Res.* **2008**, *1*, 203–212. (d) Wang, H.; Robinson, J.; Li, X.; Dai, H. *J. Am. Chem. Soc.* **2009**, *131*, 9910–9911.
(10) Eda, G.; Lin, Y.; Mattevi, C.; Yamaguchi, H.; Chen, H.; Chen, I.; Chen, C.; Chhowalla, M. *Adv. Mater.* **2010**, *22*, 505–509.
(11) Xiao, L.; Yang, Y.; Yin, J.; Li, Q.; Zhang, L. *J. Power Sources* **2009**, *194*, 1089–1093.

JA105296A